J Paleolimnol (2017) 57:37–49
DOI 10.1007/s10933-016-9925-z

ORIGINAL PAPER

Effects of spring warming and mixing duration on diatom deposition in deep Tiefer See, NE Germany

Ulrike Kienel · Georgiy Kirillin · Brian Brademann · Birgit Plessen · Reinhard Lampe · Achim Brauer

Received: 1 April 2016 / Accepted: 19 October 2016 / Published online: 27 October 2016

Abstract Monitoring during three meteorologically different spring seasons in 2012, 2013, and 2014 revealed that temperature increase in spring, which influences spring lake mixing duration, markedly affected nutrient availability and diatom deposition in a sediment trap close to the bottom of deep Tiefer See, NE Germany. Deposition of *Stephanodiscus* taxa and small *Cyclotella* taxa was much higher after late ice out and a deep, short lake mixing period in spring 2013, compared to that after gradual warming and lengthy lake mixing periods in spring 2012 and 2014, when only brief or marginal ice cover occurred. Availability of dissolved Si and P was 33 and 20 % higher, respectively, in 2013 compared to 2014. The observed relation between high (low) diatom deposition and short (lengthy) mixing duration in spring was applied to varved sediments deposited between AD 1924 and 2008. Low detrital Si content in trapped material and a sediment core enabled use of µXRF-counts of Si as a proxy for diatom silica. The spring mixing duration for 1951–2008 was derived from FLake-model calculations. The spring warming duration related to lake mixing was approximated from air temperatures for 1924–2008 using the dates when daily mean air temperature exceeded 5 °C (start) and 10 °C (end). Diatom silica deposition showed a significant ($p < 0.0001$) inverse linear relationship with the modeled spring mixing duration ($R^2 = 0.36$) and the spring warming duration ($R^2 = 0.28$). In both cases, the relationship is strengthened when data from the period of low diatom production (1987–2005) is excluded ($R^2 = 0.59$ and $R^2 = 0.35$). Part of this low diatom production is related to external nutrient supply that favored growth of cyanobacteria at the expense of diatoms. This approach shows that diatom Si deposition was strongly influenced by the availability of light and nutrients, related to the duration of lake mixing and warming in spring, during most of the studied period. The remaining unexplained variability, however, indicates that additional factors influence Si deposition. Further tests in other deep, temperate lakes are necessary to verify if this relation is a common feature and consequently, if diatom Si can be used as a proxy for spring mixing duration in such lakes.

Keywords Lake sediment · Lake monitoring · Diatom bloom · Spring circulation · FLake model · Deep lake

---

U. Kienel (✉) · R. Lampe
Institute for Geography and Geology, University Greifswald, Friedrich-Ludwig-Jahn-Str. 16,
17487 Greifswald, Germany
e-mail: ukienel@gfz-potsdam.de

U. Kienel · B. Brademann · B. Plessen · A. Brauer
Section 5.2 Climate and Landscape Evolution, GFZ German Research Centre for Geosciences,
Telegrafenberg, 14473 Potsdam, Germany

G. Kirillin
Leibniz-Institute of Freshwater Ecology and Inland Fisheries, Müggelseedamm 310, 12587 Berlin, Germany

Introduction

Although climate-related phenological shifts towards earlier spring events in a warming climate are broadly observed (Menzel et al. 2003; Thackeray et al. 2008; Winder et al. 2012), there remains a lack of consensus on how climate affects lake plankton production (Winder and Sommer 2012), with a variety of mechanisms proposed. Phytoplankton dynamics are basically linked to annual fluctuations in temperature, irradiance and wind, which regulate mixing and stratification of the water column that in turn changes the availability of light and nutrients for growth. In deep lakes, the onset of the spring phytoplankton bloom is coupled to the onset of thermal stratification, i.e. the transition from strong to weak turbulent mixing (Peeters et al. 2007b), which increases the mean light exposure of the cells, but limits subsequent nutrient supply (Wetzel 2001; Winder and Schindler 2004b). Studies in European lakes found that the duration of deep mixing after warmer winters decreased and earlier lake stratification promoted earlier onset of the phytoplankton bloom in spring (Weyhenmeyer et al. 2002; Peeters et al. 2007a). Phytoplankton chlorophyll concentrations in spring increased, along with a late and rapid thermal stratification (Peeters et al. 2007a), given a sufficient supply of nutrients by seasonal mixing. This is because phytoplankton production and the rate of nutrient exploitation are accelerated with an increase in light availability. The maximum biomass produced from the same nutrient pool is larger when the nutrient pool is quickly exploited because increasing numbers of cells are lost to sinking through time (Peeters et al. 2013).

The development of phytoplankton blooms is normally strongly determined by biotic interactions (Reynolds 1984; Sommer et al. 1986). For example, zooplankton grazing can terminate diatom blooms in spring through complex interactions with temperature, bloom timing and magnitude, and lake mixing (Jäger et al. 2008; Berger et al. 2010). Warmer winter/spring conditions were found to cause earlier starts and terminations of phytoplankton blooms. For example, in large and deep Lake Washington, spring stratification and the spring phytoplankton bloom advanced by 21 and 27 days, respectively, since 1962 (Winder and Schindler 2004a). The earlier phytoplankton peak led to significant declines in slower-growing *Daphnia* populations, as they were not able to adjust to these phenological changes. The mis-match between early phytoplankton blooms and a later zooplankton spring peak may further disrupt predator–prey relationships up to higher levels in the food chain (Winder and Sommer 2012). In shallow Müggelsee, diatom peak production in spring was larger and occurred earlier and at lower water temperatures after warmer winters, and the cladoceran peak was delayed (Shatwell et al. 2008). This provided an ideal opportunity for cyanobacteria to establish dominance after the diatom spring bloom of cold-adapted, smaller, centric species (Shatwell et al. 2008). Buoyant cyanobacteria are also favored over heavier, sinking diatoms in warmer, more stable water columns (Huisman et al. 2004; Jöhnk et al. 2008; Shatwell et al. 2008), with a subsequent further disadvantage for diatom populations as a result of light shading from cyanobacterial blooms at the lake surface (Dokulil and Teubner 2000). Among diatoms, small-cell species with a high surface area to volume ratio benefit from stable water conditions, as their relatively low sinking velocities enable them to remain longer in the photic zone, where they are efficient at obtaining resources such as light and nutrients (Winder et al. 2009; Rühland et al. 2015). As diatom silica content is related to biovolume (Conley et al. 1989), this size reduction may lead to a decrease in silica deposition.

In addition to the complexity of the interactions discussed so far, the lack of consensus on climate effects on plankton production may result from the compilation of data from lakes that cover large gradients in factors such as climate, water depth, morphology and trophic state conditions (Jeppesen et al. 1997; Blenckner et al. 2007), with different mixing regimes and different recycled nutrient requirements for phytoplankton production. Also, among-site differences or excessively long intervals between sampling of plankton may complicate syntheses, as lakes may not have been sampled during peak periods of phytoplankton abundance. In contrast, a continuous record of phytoplankton development can be provided by trapping lake deposition and development of the plankton can be reasonably followed using biweekly trapping periods. A direct link between the sediment trap data and the sediment record can then be established using, for instance, diatom silica calculated from diatom biovolumes (Conley et al. 1989) and silica data from the sediment, here estimated from the annual average of µXRF counts. The special case of well dated, annually laminated sediments, then enables precise comparisons of the recent sediment record with instrumental data and offers the chance to verify the observed relationships among diatom production, lake and weather conditions. Using this approach, we present sediment trap data on diatom assemblages and the Si contribution from just above the lake bottom in the deep Tiefer See, NE Germany. Data come from three consecutive years that experienced large differences in spring temperature and lake mixing conditions. Observed relations between trapped diatom silica and monitored spring warming and lake mixing were applied to a series of silica deposition data recorded in the recent varve record (1924–2008) (Kienel et al. 2013), the past lake mixing duration in spring modeled using the lake temperature model FLake (Mironov 2008), and related past spring warming derived from air temperatures. This approach allowed us to infer potential mechanisms that influence diatom production in a deep lake, and to assess whether diatom Si can be used as a proxy for spring mixing duration.

Site description

Tiefer See is located 90 km NNW of Berlin in the morainic terrain of the NE-German Polish Basin (Fig. 1a), within the tills of the Pomeranian terminal moraine (Landesamt für Umwelt, Naturschutz und Geologie Mecklenburg—Vorpommern 2000). With a maximum depth of 62.5 m, Tiefer See is the deepest lake in the N–S trending Klocksin Lake Chain (Fig. 1b; Table 1), which formed as part of a subglacial gully system. An open connection to Flacher See in the N was documented to have still existed in the eighteenth century (Engel 1961). With the construction of a dam for a railway track (1884–1886) at this site, pipes were laid to keep the lakes connected. Within the agricultural catchment of Tiefer See, the paludified area to the SE was drained by a bucket elevator between 1984 and 1995 (Water Board Müritz). Pig farming in Alt Gaarz increased after 1975 to about 15,000 animals, and manuring of the fields surrounding the lake, in turn increased the nutrient contribution to the lake. The establishment of private farming in the 1990s decreased the number of animals to approximately 1000, resulting in a decline in nutrient contribution to the lake.

Tiefer See is currently dimictic, but ice coverage is rarely observed. The mesotrophic, hard-water lake becomes oxygen deficient below 40 m water depth towards the end of summer stratification (Table 1). Climate conditions for the Tiefer See region are warm-temperate and humid. Highest average temperatures (16–18 °C) and precipitation (55–65 mm per month) are recorded during June to August. During winter (December–February), temperatures are around the freezing point and monthly precipitation is minimal in

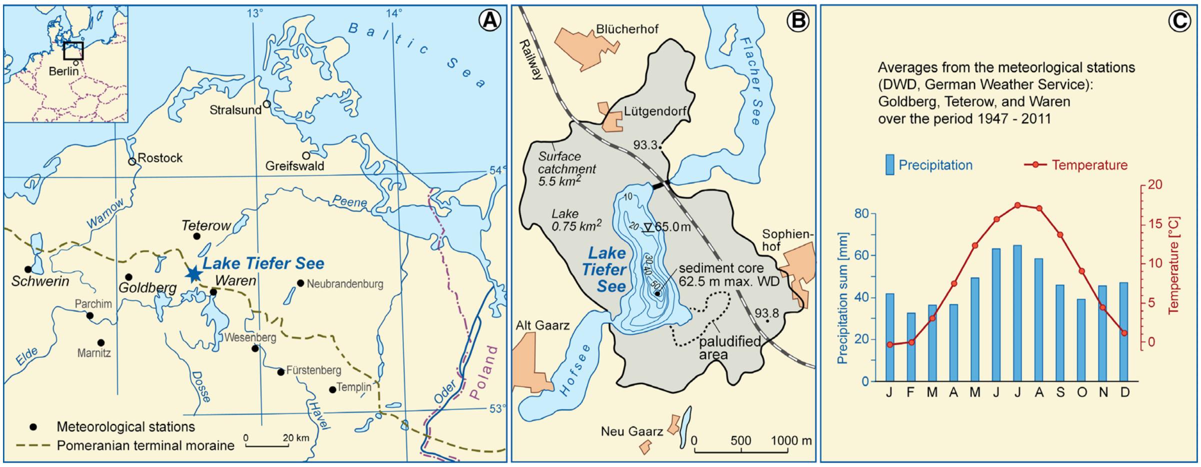

Fig. 1 Location of Tiefer See. **a** Geographic position in NE Germany, within the tills of the Pomeranian terminal moraine. **b** Tiefer See within the Klocksin Lake Chain, lake and surface-catchment areas, lake bathymetry and position of the sediment core at the site of maximum water depth (WD). Flacher See and Tiefer See are connected via pipes running through the dam constructed for the railway track. **c** Monthly mean values of temperature and precipitation averaged over the period 1947–2011

Table 1 Basic data for Tiefer See. Nutrient contents are averages for the mixed water column

Site	Tiefer See
Coordinates	53°35′N, 12°32′E
Varved sediment sequence (year AD) studied	1924–2008
Lake volume (10^6 m^3)	14
Lake area (km^2)	0.76
Lake max depth/mean depth (m)	62.5/18.5
Conductivity (μS cm^{-1}) minimum/maximum	500/560
TP (μg L^{-1})	30
TN (mg L^{-1})	1.3
Trophic status	Mesotrophic

February, with approximately 30 mm (mainly as rain) (Fig. 1c). Mean annual precipitation amounts to ~560 mm. The predominant wind direction is WSW.

Materials and methods

Monitoring of lake conditions, meteorological data and modeling

Water temperature was continuously measured since March 16, 2012 in 6-h intervals, close to the position of the greatest water depth, using 26 data loggers (HOBO Water Temp Pro v2) in 1-m steps from 0 to 15 m and in 5-m steps thereafter down to 55 m water depth. Because of technical problems, no data were collected between 4 April and 6 June 2014, and from 9 September to 18 December 2014 only monthly data were recorded.

Concentrations of dissolved silica and phosphorus were measured in water samples retrieved from 1, 3, 5, and 7 m water depths at monthly intervals during the years 2013 and 2014. The water samples were immediately filtered using 45-μm filters (Sartorius). Samples for total phosphorus (TP) determination were HNO_3-stabilized. TP and Si concentrations were determined by ICP-AES (Iris, Thermo Instrumental). Results are averages of at least two emission lines and triple measurements.

Meteorological data were taken from the Schwerin Station of the German Weather Service (DWD), 75 km W of Tiefer See. They included daily mean air temperature (available since 1890), daily sunshine duration, and daily means for cloud cover, wind speed, and relative humidity (available since 1951).

Lake water temperature and mixing depth were calculated using the lake temperature model FLake. The highly parameterized model is designed for long-term calculations of lake thermodynamics at low computational costs and with minimum adjustment (Mironov 2008), and was successfully validated for a number of lakes with similar morphological characteristics (Kirillin 2010; Kirillin et al. 2012, 2013; Thiery et al. 2014). Data input includes the daily sunshine duration and daily means for temperature, wind speed, relative humidity, and cloud cover (data set available since 1951). Further, the lake mean depth of 18.5 m and a water transparency of 3 m were used for calculations. Mixing depths were modeled in FLake based on a correlation between the predicted and measured lake surface temperatures of 0.98 (normalized standard deviation 0.92, RMS error 1.3 °C). The maximum mixing depth that can be modeled is restricted to the mean lake depth of 18.5 m. The spring mixing duration was calculated using the first day with a mixing depth >18 m after the winter cold (start) and the first day with a mixing depth <6 m (end).

A simple estimate for the spring warming related to the mixing duration was based on daily mean air temperatures (available since 1890) and calculated as the running mean temperature of the previous 5 days to account for the delay of signal transfer to the lake water. The spring warming duration was calculated from the start of deep spring mixing, which was assumed to occur on the first day that the calculated running mean air temperatures exceeded 5 °C without a temperature decrease below 3 °C afterwards, until the lake stratified, which was assumed to occur on the first day that the calculated running mean air temperatures exceeded 10 °C.

Monitoring of sediment deposition and the sediment core

An automated sediment trap with an active area of 0.125 m^2 (TECHNICAP PPS 3/3) equipped with 12 sample bottles was placed close to the lake bottom at a water depth of 50 m on 16 March 2012. Sample containers were filled with distilled water and the sampling period was set to 15 days before installing the trap. The trap was retrieved and equipped with new sample containers after 180 days. Because of technical problems, the periods from 9 to 20 September 2012 and 3–15 May 2013 were not sampled.

An 82.5-cm mud-water interface sediment core was retrieved in April 2011 from the deepest part of Tiefer See (Kienel et al. 2013) using a Ghilardi Gravity Corer (Kelts et al. 1986). Above faintly laminated sediments, the top 38 cm are composed of alternating mm-scale, light calcite laminae with thicker, dark-brown organic-rich layers. The varve character of these laminations was established by analyses of thin sections from epoxy-resin-impregnated sediment blocks prepared following standard procedures (Brauer and Casanova 2001). Continuous seasonal layers were measured and counted to cover the period AD 1924–2010 without counting error (Kienel et al. 2013).

Micro-XRF element scans were performed with an Itrax core scanner using a Mo-tube (voltage 30 kV, current 30 mA) at constant distance from the foil-covered surface of the split cores (Croudace et al. 2006). Measuring step size and exposure time were 200 µm and 10 s, respectively. Because of the requirements of measurement geometry, the top 5 mm of the core were not measured, reducing the period covered by element data to AD 1924–2008.

The match of the calcite layers with the Ca-peak counts facilitated transfer of the µXRF element data to the varve sublayers measured on thin sections. The start of a varve year is marked in the element data by increased Si counts, reflecting the spring diatom bloom, followed by a distinct Ca peak, indicating calcite deposition. The latter is separated from the spring Si increase of the following varve by a mixed signal of lower Si, Ca, and elevated Ti and K counts, reflecting low productivity and reworking. Annual mean counts were calculated for Si by averaging the measured count rate over the respective annual layer.

Trap-sample preparation and analyses

The trap samples were freeze-dried and weighed to determine areal dry deposition per day. For microscopic inspection of the diatom concentration and assemblage, each sample was homogenized. For each preparation, an aliquot of 2 mg of the homogenized sample was suspended in 5 ml of purified water using mild ultrasonic treatment. Microspheres (stock solution prepared by V. Jones, University College London) were added to the suspended sample until similar amounts of diatoms and microspheres were reached. An aliquot of 400 µL of the sample was spread over a round cover slip, allowed to dry over night at room temperature, and mounted with Naphrax (refractive index 1.73). For each sample, the diatom valves along with 500 microspheres were counted using a Zeiss Axioskop 2 plus, at 630× magnification. Diatom concentration was then calculated using the number of enumerated microspheres (Battarbee and Kneen 1982). The identification of diatoms followed Krammer and Lange-Bertalot (1991). Describing authorities for the important taxa are given in Table 2.

Carbon and nitrogen contents were determined using 1-mg aliquots of ground, freeze-dried sediment samples. Total carbon and nitrogen contents (TC and TN) were analyzed from aliquots weighed in Sn capsules, using an elemental analyzer (EA3000-CHNS Eurovector). Prior to determination of total organic carbon and nitrogen (TOC, TON) 1-mg-sample aliquots were decalcified in Ag capsules (20 % HCl and drying at 75 °C). The TOC content was measured in an elemental analyzer (NC2500). $CaCO_3$-carbon contents were calculated from the difference of TC and TOC. Accordingly, the portions of the deposition can be classified as percentages of organic

Table 2 Important diatom species and taxonomic references in Krammer and Lange-Bertalot (1991)

Species	Reference
Aulacoseira islandica	(O. Müller) Simonsen 1979
Cyclotella comensis	Grunow in van Heurck 1882
Stephanodiscus neoastrea	Håkansson and Hickel 1986
Stephanodiscus parvus	Stoermer and Håkansson 1984
Fragilaria crotonensis	Kitton 1869
Asterionella formosa	Hasall 1850

matter (OM), $CaCO_3$, and non-carbonate inorganic matter (IM), which includes the siliceous diatom frustules. This diatom-Si portion of the trapped sediments was estimated using the relation $\log_{10}$ [silica content] $= 1.03 \times \log_{10}$ [diatom biovolume] $- 2.45$, according to which the silica content of diatoms is related to their biovolume (Conley et al. 1989). Biovolumes and Si contents of the major diatom taxa are given in Table 3.

Results

Trapped deposits and their characteristics

The sediment trap samples (15-day increments) showed the maximum sediment deposition occurred in spring in all years and a secondary maximum occurred in summer in 2012 and 2013. The summer deposition maxima were similar, with 4 to 5 g d^{-1} m^{-2}, but the spring maximum deposition was significantly higher in 2013 compared to 2012 and 2014 (Fig. 2). Non-carbonate IM deposition in 2013 was also significantly higher compared to that in 2012 and 2014. Deposition rates during winter were lower in 2012/2013 than in 2013/2014 and very low amounts of diatoms were found in this material.

The most common diatom species recorded were *Aulacoseira islandica*, small benthic *Fragilaria* (sensu lato), *Fragilaria crotonensis*, *Asterionella formosa*, *Cyclotella comensis*, *Stephanodiscus neoastrea* and *S. parvus*. Diatom deposition [diatoms d^{-1} m^{-2}] reached highest values in spring 2013 with 19.8×10^9 diatoms d^{-1} m^{-2}. The diatom deposition peaks in spring and summer 2012 and in summer 2013 reached values between 2 and 3×10^9 diatoms d^{-1} m^{-2}, whereas the spring peak of diatom deposition in 2014 amounted to only 0.6×10^9 diatoms d^{-1} m^{-2}. The small benthic *Fragilaria* (sensu lato), *A. islandica* and *A. formosa* occurred mainly in spring. *Fragilaria crotonensis* occurred in summer and reached comparable amounts in 2012 and 2013, but was suppressed in 2014. *S. neoastrea*, *S. parvus*, and *C. comensis* occurred mainly in spring in 2012 and 2014, but in 2013 they also occurred in early summer. The greatest difference among the 3 years however, was that in spring 2013 there were notably higher deposition rates of *S. neoastrea*, *S. parvus* and *C. comensis*.

To test whether μ-XRF counts of Si can be used as a proxy for the amount of diatoms or if these data are biased by significant contributions of detrital silica, we calculated the diatom-silica deposition in the traps using the average biovolumes of the dominant diatom species (Table 3) (Conley et al. 1989). The calculated diatom Si was found to clearly determine the deposition of non-carbonate inorganic matter (IM), with on average 77 % of IM and an explained variability of 80 % (Fig. 3). This indicates a low detrital input of silica and that μ-XRF-counts of Si are a suitable proxy for the diatom contribution. The calculated Si deposition was highest in 2013, followed by that in 2012 and 2014. The calculations further show that the differences in the silica contributions relate most strongly to the blooms of *Stephanodiscus* sp. and *C. comensis*.

Lake and weather conditions

The weather and lake conditions during the transition from winter to spring differed strongly among the three years (Fig. 3). A long period of frost and a (partial) lake-ice cover from 15 January until 15 April 2013 differed markedly from shorter frost periods in January/February 2012 and in January 2014, when only partial or marginal ice cover developed. Spring warming in 2013, following a long frost period with inverse lake stratification, occurred very quickly. Within 5 days, air temperature increased to 5 °C and

Table 3 Biovolumes and Si contents of the major diatom taxa calculated according to Conley et al. (1989)

Species	Biovolume (μm^3)	Si content (μmol cell^{-1})	Si content (pg cell^{-1})
A. islandica	3600	20.1	562
C. comensis	300	3.7	103
S. neoastrea	16,700	55.0	1545
S. parvus	1600	13.2	371
F. crotonensis	750	6.0	169
A. formosa	520	4.7	132

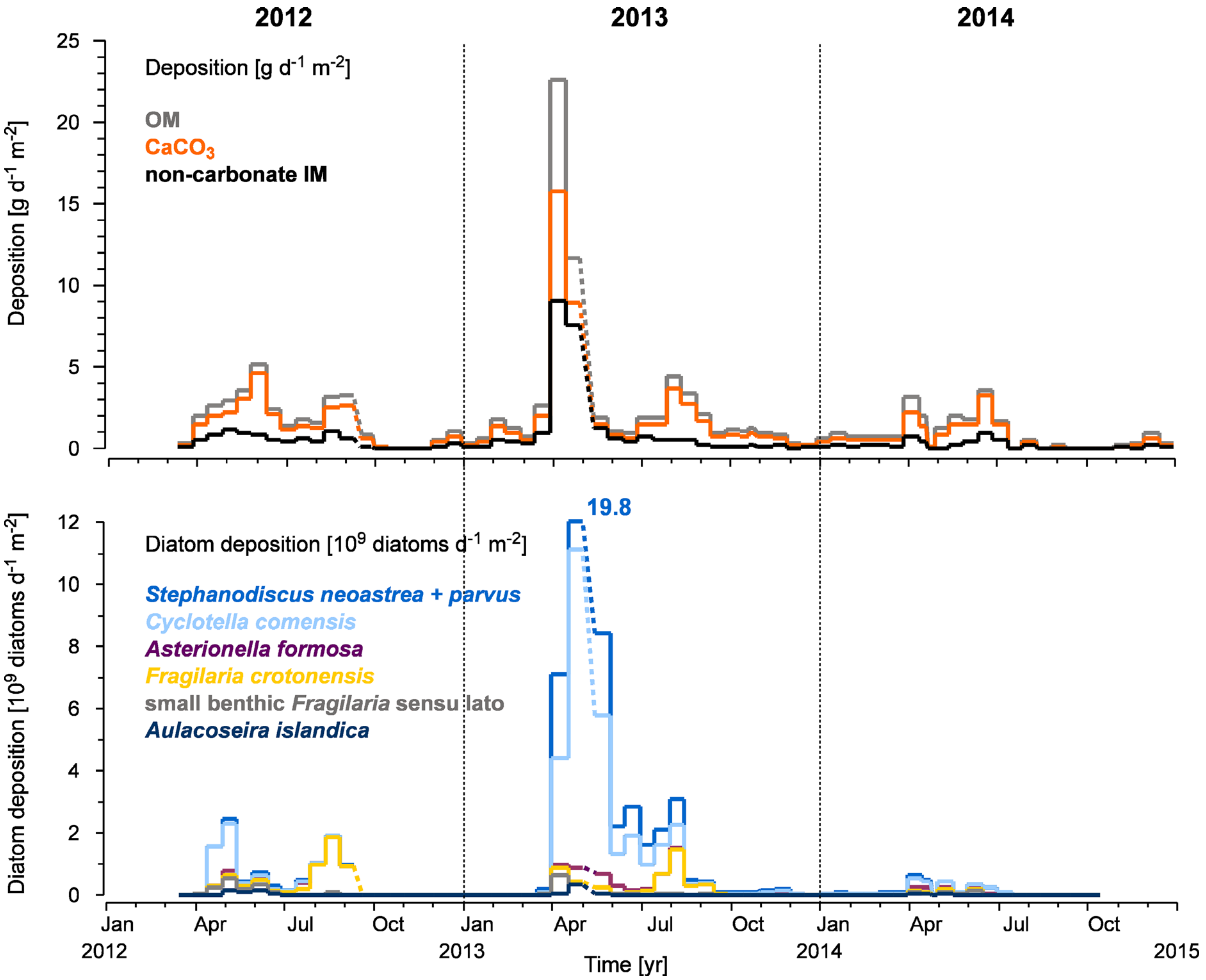

Fig. 2 Trapped hypolimnion deposition (*upper panel*) from March 2012 to October 2014 in 15-day increments, and proportions of organic matter (OM), calcite ($CaCO_3$), and non-carbonate inorganic matter (IM). *Lower panel* is the same, but for diatoms, including the assemblage composition of major taxa. (Color figure online)

exceeded 10 °C after an additional five days, causing the ice cover to melt and promotion of deep mixing of the water column (modeled mixing depth >18 m). This was followed by the rapid onset of thermal stratification (modeled mixing depth <6 m) that was facilitated by a period of decreased wind speed at the end of April. The deep mixing started on day 103 and stratification started on day 127 in 2013. In contrast, spring warming in 2012 and 2014 started earlier, was gradual, and led to earlier onsets of deep mixing (on days 83 and 57, respectively) and the lake stratified on days 114 and 117, respectively, following short periods of lower wind speeds. The spring mixing duration (calculated from the FLake model estimates according to Mironov (2008)) from the onset of deep mixing >18 m depth, to stratification with a mixing depth <6 m, was determined to be 42 days in 2012, 25 days in 2013, and 61 days in 2014 (Fig. 3). The rise of air temperature above 5 °C promoted the mixing of the water column after the winter cold. Following an air temperature rise above 10 °C, the lake stratified and the deposition of diatom Si increased. Using these air temperature criteria, the spring warming duration was determined to be 47 days in 2012, 5 days in 2013, and 57 days in 2014 (Fig. 3). In each case, we hypothesize an inverse relation between diatom silica deposition and the duration of both lake mixing and warming in spring.

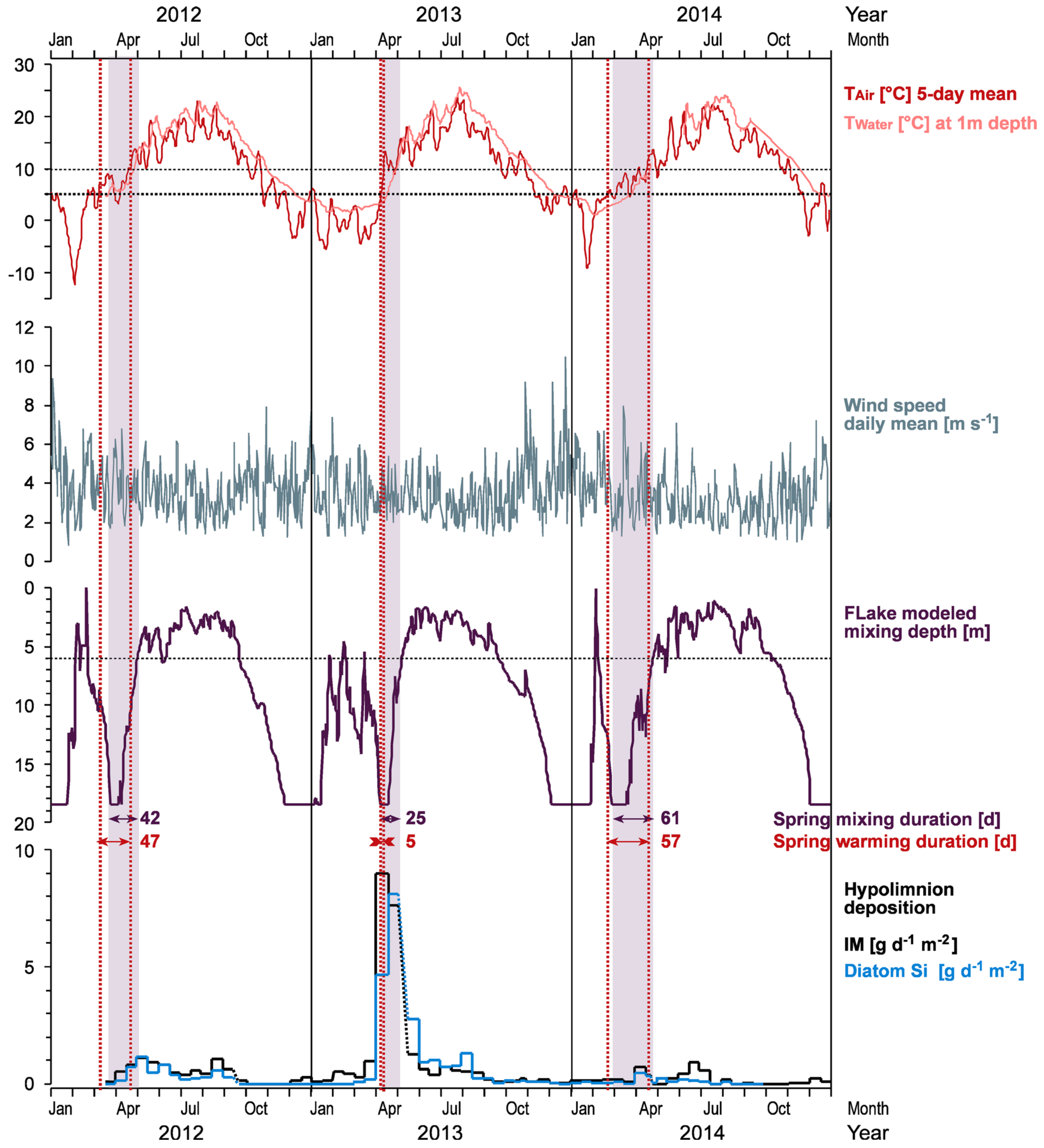

Fig. 3 Lake water and climate conditions for the period 2012–2014, including water temperature, air temperature with running means of the previous 5 days, and wind speed. Also shown are the mixing depth calculated using the lake temperature model FLake (Mironov 2008), along with Si deposition calculated from diatom biovolumes according to Conley et al. (1989), which is correlated with the trapped deposition of non-carbonate inorganic matter (IM). The *vertical shaded areas* indicate the spring mixing durations (estimated from the modeled mixing depth), and the *vertical dotted lines* indicate the spring warming durations (related to lake mixing and estimated from air temperature criteria)

Concentrations of dissolved Si and P, important diatom nutrients, are available for 2013 and 2014 only (Fig. 4). Concentrations of these nutrients during spring mixing, and available for the diatom spring bloom, were higher in 2013 than in 2014, with 33 % more Si and 20 % more P.

Fig. 4 Concentrations of dissolved silica and phosphorus measured in the water column at depths of 1, 3, 5 and 7 m for 2013 and 2014. The concentrations of these nutrients were in both years, higher during the mixing period, but decreased when the phytoplankton blooms started and remained low during the stratification period. In 2013, before the onset of the diatom spring blooms, the Si concentration was 33 % higher than in 2014 and the P concentration was 20 % higher than in 2014

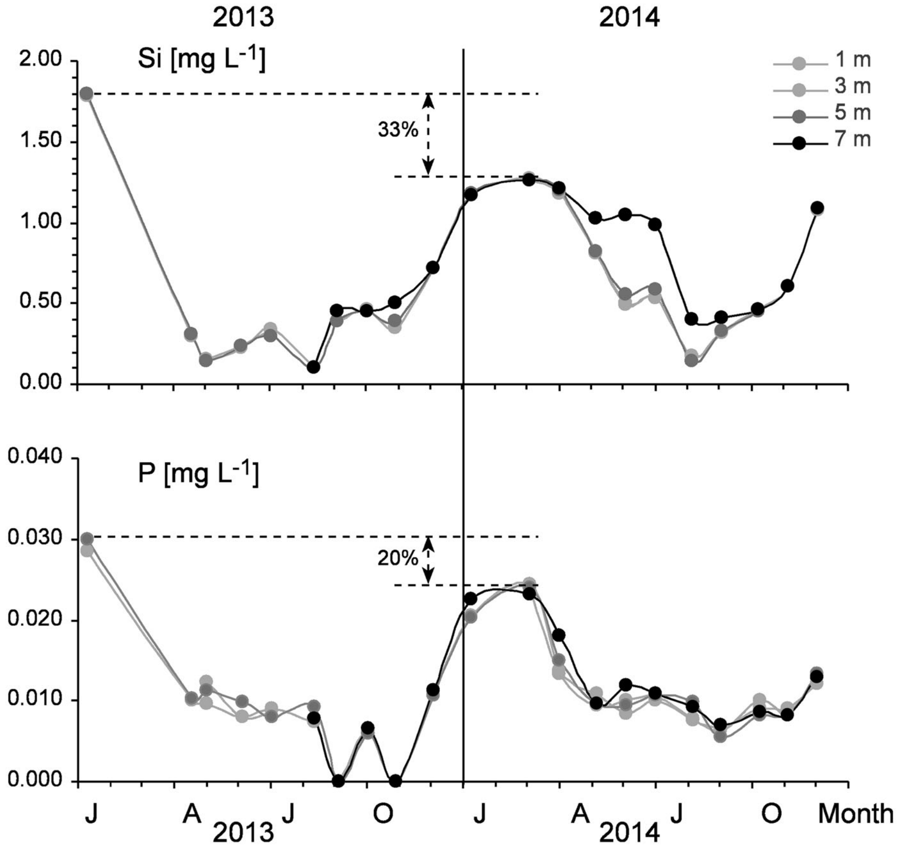

Extending the test of monitoring observations back in time

To determine whether the observed effect of the duration of spring warming (i.e. the number of days for air temperature to rise from 5 to 10 °C) and spring mixing (i.e. the number of days between the onset of deep mixing >18 m depth to stratification with a mixing depth <6 m) on diatom production was a random phenomenon in our observation period, we analyzed the diatom deposition in varved sediment which formed since AD 1924 in Tiefer See (Kienel et al. 2013).

The calculated diatom Si deposition during the three years of monitoring data suggests a clear dominance of diatom Si over detrital Si and 70 % of the diatom Si collected in the sediment traps was derived from the spring diatom bloom. This suggests that: (1) the µXRF-counts of Si measured continuously along the varved sequence can be used as a proxy for diatom deposition, and (2) the annual average count rate of Si is a robust measure for the annual diatom deposition in Tiefer See (Fig. 5). According to the annual mean µXRF counts of Si, diatom deposition tended to decrease after 1970, reached lowest values and inter-annual variability after 1987, and returned to higher values after 2005.

For the varved period of 1951–2008 in the sediment core, the inferred duration of spring mixing estimated by the FLake model (spring mixing duration) explains 36 % of the variability in diatom Si (Fig. 5). The percentage explained increased to 59 % when the period with low diatom Si values (1987–2005) was removed from the data set prior to regression analysis. To extend this test to the varved period from 1924 to 2008, we used a simple temperature estimate related to the duration of mixing (spring warming duration). In this case, 28 % of the variability in diatom Si is explained for the entire period, and this increases to 35 % when the period 1987–2005 is removed from the data set (Fig. 5). All correlations are significant at $p < 0.0001$. We also tested for the influence of the

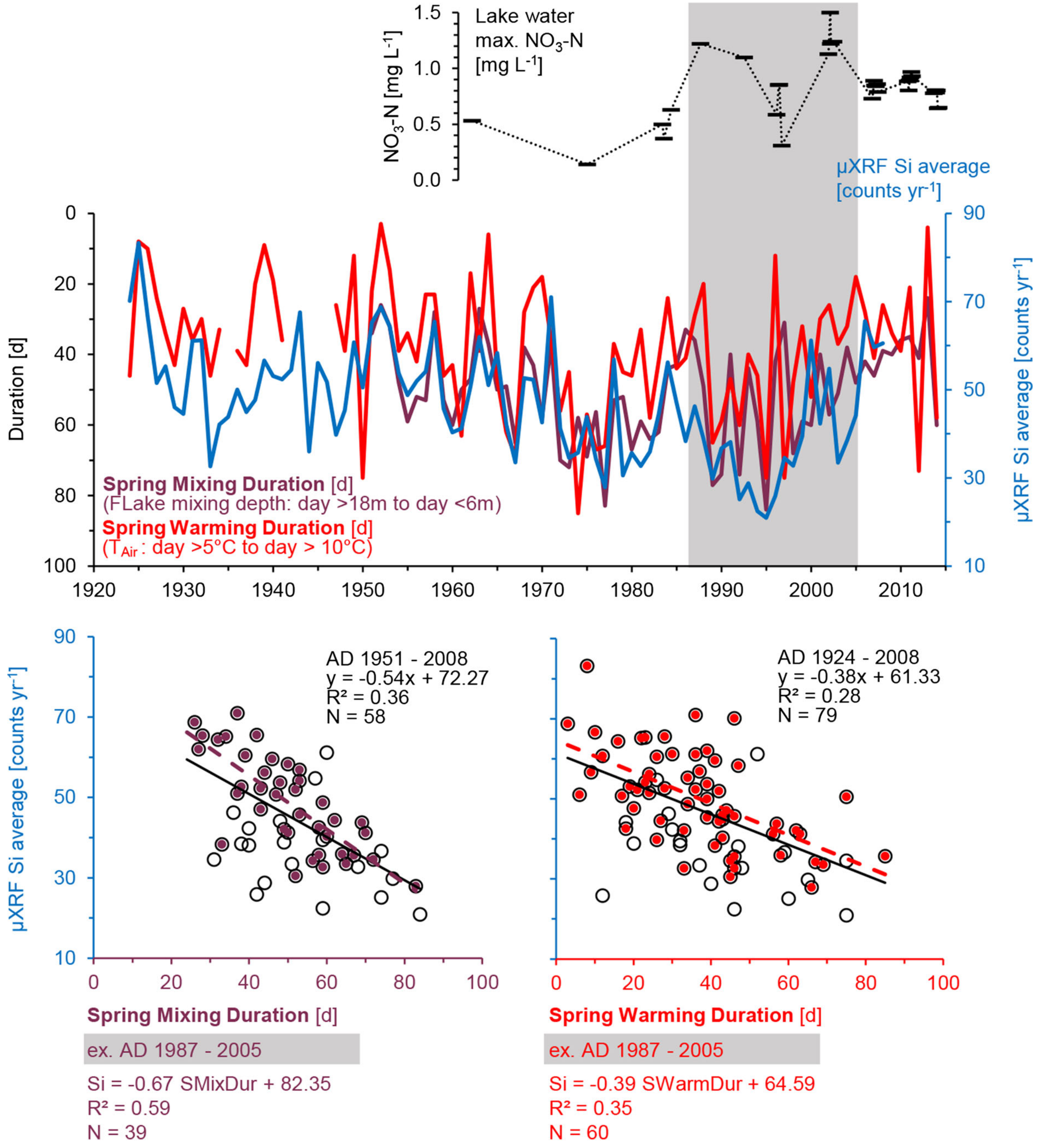

Fig. 5 Diatom Si measured in the varved sediment core from Tiefer See, calculated as the annual average of µXRF Si counts, compared to the spring mixing duration calculated from FLake-modeled mixing depths and the spring warming duration calculated from the Schwerin temperature series (*upper panel*). The *shaded area* denotes the period of increased nutrient concentration when the deposition of diatom Si is low. The *lower panels* show the regression of the Si data on the spring mixing and warming durations. *Lower left* spring mixing duration calculated with FLake for the whole data set 1951–2008 (*black*, *empty circles* and *trend line*) and of the reduced data, excluding the period 1987–2005 (*violet*, *filled circles* and *trend line*). *Lower right* spring warming duration of the whole data set 1924–2008 (*black*, *empty circles* and *trend line*) and reduced data set (see above) (*red*, *filled circles* and *trend line*). The regression equations and explained variability are indicated and all are significant at $p < 0.0001$. (Color figure online)

timing of the end of deep mixing and the onset of stratification, and the timing of air temperatures exceeding 5 and 10 °C on the diatom Si deposition. In all cases, correlations were not significant.

Discussion

The observed clear increase in diatom deposition in Tiefer See during spring 2013 occurred after late, rapid ice out, a deep, but short mixing of the water column, and a rapid onset of stratification, mediated by a rapid warming in mid-April. Both the start of deep mixing and the onset of stratification occurred later than in 2012 and 2014. The duration of the period of spring mixing in 2013 was, however, shorter than in 2012 and 2014. This relation was similar when the increase in air temperature above 5 °C and above 10 °C was used as the criterion, and the duration of the spring warming period was shortest in 2013 (Fig. 3). Deep mixing can recycle nutrients including those released from the sediment under anoxic conditions (Reynolds 1984; Smayda 1969; Wetzel 2001). During spring 2013 at Tiefer See, this scenario likely resulted in elevated concentrations of nutrients (Si and P, Fig. 4) that offset nutrient limitation for algal production, an occurrence commonly reported in deep lakes (Jäger et al. 2010; Peeters et al. 2013). In addition to high nutrient availability, the diatoms benefited from the rapid onset of stratification that increased the intensity of incident light. This explanation is supported by modeling results from deep Lake Constance where the maximum biomass produced from the same nutrient pool was modeled to be larger, the faster the nutrient pool was exploited, because of the increased losses of phytoplankton to sedimentation with time (Peeters et al. 2013). The pattern of peak phytoplankton concentrations following late and rapid stratification was also observed in Lake Constance (Peeters et al. 2007a). An additional factor favoring spring diatom peaks may be derived from the competitive advantage of diatoms that bloom under the ice (Vehmaa and Salonen 2009). Although this has been observed for *Aulacoseira islandica* in other lakes (Bradbury et al. 2004), in Tiefer See *Stephanodiscus* species and *Cyclotella comensis* seem to have strongly benefitted from growing under ice (Fig. 2).

In contrast to 2013, spring mixing lasted longer and was shallower in 2012 and 2014, resulting in less nutrients being recycled from depth (assumed for 2012 and measured for 2014), thereby delaying and weakening the development of the spring bloom as diatom cells were mixed below the photic depth.

The percentage of variability of diatom Si in the sediment (AD 1924–2008) explained by the mixing duration (36 %) and the warming duration (28 %), indicates that there are additional factors that determine the development of diatom production and deposition. If, however, the period of low diatom deposition (AD 1987–2005) is removed from the dataset, the percentage of explained variability increases to 59 % for mixing duration and 35 % for warming duration (Fig. 5). The excellent diatom preservation, together with lower individual numbers, demonstrates that the decreased silica deposition is not a function of poor preservation. Documented, synchronous increases in livestock in the catchment and field drainage suggest that manure may be the source of additional nutrients (Kienel et al. 2013). An increase in nutrient concentrations during the period of low diatom deposition is confirmed by increased concentrations of nitrate nitrogen measured in the lake (Fig. 5) (Data from Ministry of Agriculture, Environment, and Consumer Protection Mecklenburg-Pomerania). In addition to the increase in nutrient concentrations in the mid-1980s, the first 5 °C-day after the winter cold tended to occur earlier from then on, which is in agreement with the widely observed spring warming trend. It is plausible that in Tiefer See, an increase in nutrient concentration and an earlier onset of spring warming may have caused the observed decrease in deposition of diatom Si. Increased nutrient availability and a warmer and more stable water column provide a competitive advantage for buoyant cyanobacteria over negatively buoyant diatoms (Huisman et al. 2004). In addition, this can lead to light shading of diatoms by cyanobacteria such as *Limnothrix redekei*, which occurs throughout the epilimnion of lakes (Dokulil and Teubner 2000). As a modern analog, we observed a strong bloom of *L. redekei*, (particulate matter 12 mg L^{-1} at maximum) following weak diatom deposition in mid-May after the gradual spring warming in 2014 (warming duration = 57 days). Consistent with our findings, there is increasing evidence that organic compounds of N are important for bloom development of non-N-fixing cyanobacteria such as *L. redekei* (Davis et al. 2010; O'Neil et al. 2012; Posch et al. 2012; Paerl and Otten

2013). Also, the success of smaller, less silicified diatoms in warmer waters with more stable stratification (Winder et al. 2009), can lead to a decrease of silica deposition simply because their biovolumes and consequently their silica contents are smaller (Conley et al. 1989). Eventually, phytoplankton blooms tend to be weaker when starting and end earlier in the context of earlier and stronger zooplankton peaks (Jäger et al. 2008; Berger et al. 2010).

In conclusion, our observations from 2012 to 2014 indicate an inverse relation between the deposition of diatom silica and the duration of warming and lake mixing in spring. To evaluate these relations, we used the deposition of diatom silica (with annual mean µXRF counts of silica as a proxy for diatoms) and calculations of spring warming and mixing durations, using air temperature criteria and mixing depths calculated with the FLake model. Both relations are stronger when the period 1987–2005, with low diatom Si deposition and increased nutrient inputs from manuring of the agricultural catchment, was excluded from the regression. In Tiefer See, diatom silica deposition was not affected by the duration of spring mixing during this period, when warmer conditions led to a more stable water column. In conjunction with the increased nutrient concentrations, this likely caused a shift in dominance from diatoms to buoyant cyanobacteria. From 2005 onwards, the diatom—mixing response recurred, concomitant with the reduction of field drainage and livestock numbers, which resulted in lower nitrogen concentrations in the lake water.

In summary, we showed that during most years in the period 1924–2008, diatom Si deposition in deep Tiefer See was strongly influenced by the availability of light and nutrients, related to the duration of warming and lake mixing in spring, as controlled by the duration of the winter cold and the rapidity of subsequent warming. Remaining unexplained variability, however, indicates that additional factors influence Si deposition. Further tests in other lakes are necessary to test if this relation is a common feature of deep, temperate, oligo-mesotrophic water bodies or if this is a localized phenomenon observed only at Tiefer See.

Acknowledgments We thank Nadine Dräger, Miriam Groß-Schmölders, Sylvia Pinkerneil, Nicolas Werner, and a number of internship students for help with field and laboratory work. Georg Schettler is acknowledged for water chemistry analyses. We thank both reviewers for important comments and suggestions that improved the paper. This study is a contribution to the Virtual Institute of Integrated Climate and Landscape Evolution Analyses (ICLEA), Grant Number VH-VI-415. The monitoring equipment used in this study was funded by the Terrestrial Environmental Observatory Infrastructure initiative of the Helmholtz Association (TERENO Observatory NE Germany). Additional financial support was provided by the project “TSK Link” (BR 2208/11-1; LA 1029/6-1) funded by the “Deutsche Forschungsgemeinschaft” (DFG). All data files are provided by the corresponding author and can be accessed at http://teodoor.icg.kfa-juelich.de/igb3seachportal2/index.jsp and at http://www.iclea.de.

References

Battarbee R, Kneen MJ (1982) The use of electronically counted microspheres in absolute diatom anaysis. Limnol Oceanogr 27:184–188

Berger SA, Diehl S, Stibor H, Trommer G, Ruhenstroth M (2010) Water temperature and stratification depth independently shift cardinal events during plankton spring succession. Glob Change Biol 16:1954–1965

Blenckner T, Adrian R, Livingstone DM, Jennings E, Weyhenmeyer GA, George DG, Jankowski T, Järvinen M, Aonghusa CN, Nõges T, Straile D, Teubner K (2007) Large-scale climatic signatures in lakes across Europe: a meta-analysis. Glob Change Biol 13:1314–1326

Bradbury JP, Colman SM, Reynolds RL (2004) The history of recent limnological changes and human impact on Upper Klamath Lake, Oregon. J Paleolimnol 31:151–165

Brauer A, Casanova J (2001) Chronology and depositional processes of the laminated sediment record from Lac d‘Annecy, French Alps. J Paleolimnol 25:163–177

Conley DJ, Kilham SS, Theriot EC (1989) Differences in silica content between marine and freshwater diatoms. Limnol Oceanogr 34:205–213

Croudace IW, Rindby A, Rothwell RG (2006) ITRAX: description and evaluation of a new multi-function X-ray core scanner. Geol Soc Lond Spec Publ 267:51–63

Davis TW, Harke MJ, Marcoval M, Goleski J, Orano-Dawson C, Berry DL, Gobler CJ (2010) Effects of nitrogenous compounds and phosphorus on the growth of toxic and non-toxic strains of Microcystis during cyanobacterial blooms. Aquat Microb Ecol 61:149

Dokulil M, Teubner K (2000) Cyanobacterial dominance in lakes. Hydrobiologia 438:1–12

Engel F (1961) Blatt 24 Krakow am See der Wiebekingschen Karte. Historischer Atlas von Mecklenburg, Wiebeking, CF (1755–1788) Böhlau, Köln, Graz

Huisman J, Sharples J, Stroom JM, Visser PM, Kardinaal WEA, Verspagen JMH, Sommeijer B (2004) Changes in turbulent mixing shift competition for light between phytoplankton species. Ecology 85:2960–2970

Jäger CG, Diehl S, Matauschek C, Klausmeier CA, Stibor H (2008) Transient dynamics of pelagic producer-grazer systems in a gradient of nutrients and mixing depths. Ecology 89:1272–1286

Jäger CG, Diehl S, Emans M (2010) Physical determinants of phytoplankton production, algal stoichiometry, and vertical nutrient fluxes. Am Nat 175:E91–E104

Jeppesen E, Jensen JP, Søndergaard M, Lauridsen T, Pedersen LJ, Jensen J (1997) Top-down control in freshwater lakes: the role of nutrient state, submerged macrophytes and water depth. Hydrobiologia 342(343):151–164

Jöhnk KD, Huisman JEF, Sharples J, Sommeijer BEN, Visser PM, Stroom JM (2008) Summer heatwaves promote blooms of harmful cyanobacteria. Glob Change Biol 14:495–512

Kelts K, Briegel U, Ghilardi K, Hsü K (1986) The limnogeology-ETH coring system. Schweiz Z Hydrol 48:104–115

Kienel U, Dulski P, Ott F, Lorenz S, Brauer A (2013) Recently induced anoxia leading to the preservation of seasonal laminae in two NE-German lakes. J Paleolimnol 50:535–544

Kirillin G (2010) Modeling the impact of global warming on water temperature and seasonal mixing regimes in small temperate lakes. Boreal Environ Res 15:279–293

Kirillin G, Leppäranta M, Terzhevik A, Granin N, Bernhardt J, Engelhardt C, Efremova T, Golosov S, Palshin N, Sherstyankin P, Zdorovennova G, Zdorovennov R (2012) Physics of seasonally ice-covered lakes: a review. Aquat Sci 74:659–682

Kirillin G, Shatwell T, Kasprzak P (2013) Consequences of thermal pollution from a nuclear plant on lake temperature and mixing regime. J Hydrol 496:47–56

Krammer K, Lange-Bertalot H (1991) Bacillariophyceae (Centrales, Fragilariaceae, Eunotiaceae). Fischer, Stuttgart, p 576

Menzel A, Jakobi G, Ahas R, Scheifinger H, Estrella N (2003) Variations of the climatological growing season (1951–2000) in Germany compared with other countries. Int J Climatol 23:793–812

Mironov DV (2008) Parameterization of lakes in numerical weather prediction. Description of a lake model, vol 11. COSMO Technical Report. Deutscher Wetterdienst, pp 1–41

O'Neil J, Davis TW, Burford MA, Gobler C (2012) The rise of harmful cyanobacteria blooms: the potential roles of eutrophication and climate change. Harmful Algae 14:313–334

Paerl H, Otten T (2013) Harmful cyanobacterial blooms: causes, consequences, and controls. Microb Ecol 65:995–1010

Peeters F, Straile D, Lorke A, Livingstone DM (2007a) Earlier onset of the spring phytoplankton bloom in lakes of the temperate zone in a warmer climate. Glob Change Biol 13:1898–1909

Peeters F, Straile D, Lorke A, Ollinger D (2007b) Turbulent mixing and phytoplankton spring bloom development in a deep lake. Limnol Oceanogr 52:286–298

Peeters F, Kerimoglu O, Straile D (2013) Implications of seasonal mixing for phytoplankton production and bloom development. Theor Ecol 6:115–129

Posch T, Koster O, Salcher MM, Pernthaler J (2012) Harmful filamentous cyanobacteria favoured by reduced water turnover with lake warming. Nat Clim Change 2:809–813

Reynolds CS (1984) The ecology of freshwater phytoplankton. Cambridge University Press, Cambridge, p 384

Rühland K, Paterson A, Smol JP (2015) Lake diatom responses to warming: reviewing the evidence. J Paleolimnol 54:1–35

Shatwell TOM, Köhler J, Nicklisch A (2008) Warming promotes cold-adapted phytoplankton in temperate lakes and opens a loophole for Oscillatoriales in spring. Glob Change Biol 14:2194–2200

Smayda TJ (1969) Some measurements of the sinking rate of fecal pellets. Limnol Oceanogr 14:621–625

Sommer U, Gliwicz ZM, Lampert W, Duncan A (1986) The PEG-model of seasonal succession of planktonic events in fresh waters. Arch Hydrobiol 106:433–471

Thackeray SJ, Jones ID, Maberly SC (2008) Long-term change in the phenology of spring phytoplankton: species-specific responses to nutrient enrichment and climatic change. J Ecol 96:523–535

Thiery W, Martynov A, Darchambeau F, Descy JP, Plisnier PD, Sushama L, van Lipzig NPM (2014) Understanding the performance of the FLake model over two African Great Lakes. Geosci Model Dev 7:317–337

Vehmaa A, Salonen K (2009) Development of phytoplankton in Lake Pääjärvi (Finland) during under-ice convective mixing period. Aquat Ecol 43:693–705

Wetzel RG (2001) Limnology. Academic Press, San Diego, p 1006

Weyhenmeyer GA, Adrian R, Gaedke U, Livingstone DM, Maberly SC (2002) Response of phytoplankton in European lakes to a change in the North Atlantic Oscillation. Int Ver The 28:1436–1439

Winder M, Schindler DE (2004a) Climate change uncouples trophic interactions in an aquatic ecosystem. Ecology 85:2100–2106

Winder M, Schindler DE (2004b) Climatic effects on the phenology of lake processes. Glob Change Biol 10:1844–1856

Winder M, Sommer U (2012) Phytoplankton response to a changing climate. Hydrobiologia 698:5–16

Winder M, Reuter JE, Schladow SG (2009) Lake warming favours small-sized planktonic diatom species. Proc R Soc B Biol Sci 276:427–435

Winder M, Berger S, Lewandowska A, Aberle N, Lengfellner K, Sommer U, Diehl S (2012) Spring phenological responses of marine and freshwater plankton to changing temperature and light conditions. Mar Biol 159:2491–2501